

201980: gold nugget, Silica Hills (Tozer Formation, Sholl Terrane)

Sample type	Gold nugget
Total weight	1.2 g
Sample location	Silica Hills, about 25 km south of Karratha
Coordinates	Zone 50, MGA 492350E 7684225N
Datum	GDA94
1:250 000 map sheet	DAMPIER (SF 50-2)
1:100 000 map sheet	DAMPIER (2256)
Tenement	M 47/232
Collector	Artemis Resources Limited



Location and sampling

The sample was provided by Artemis Resources Limited in January 2019. It was collected from the weathering profile above quartz-veined felsic volcanic rocks at the Silica Hills prospect, in the northwest Pilbara region (Artemis Resources Limited, 2019, written comm., 11 January).

Geological context

The Silica Hills prospect is located about 4 km south of the Sholl Shear Zone, a significant terrane-boundary in the Sholl greenstone belt of the Sholl Terrane of the northwest Pilbara Craton, (Hickman, 2016; GSWA, 2020). The local bedrock comprises metamorphosed rhyolite and dacite of the 3128–3116 Ma Tozer Formation (compiled out of the GSWA 1: 100 000 scale geology map; GSWA, 2020). Metamorphosed basalt and basaltic andesite of the Tozer Formation (Hickman, 2021) outcrop immediately north of the sample locality. Proterozoic dolerite dykes transect the area (GSWA, 2020).

Gold mineralization in the area typically occurs in residual to eluvial and alluvial deposits, and in quartz -vein (e.g. Silica Hills, Sholl Northeast 2 Eluvial, Mt Sholl Dryblowing 1, Mt Sholl B1 East [Cu], and Specimen). Eluvial gold and gold-in-soil geochemical anomalies appear to have been derived from small, shallowly dipping quartz veins along lithological contacts (Bob Clynych and Associates, 1988). High -grade gold mineralization discovered in 2017 by Artemis Resources Limited at Silica Hills consists of coarse nuggetty gold with high silver content in a quartz vein stockwork within a silicified intrusion along a shear zone (Artemis Resources Limited, 2017).

The nearest regolith landforms are a colluvial unit comprising unconsolidated sand, silt, and gravel in outwash fans, scree and talus, proximal mass-wasting deposits, and an alluvial-fluvial unit comprising unconsolidated sand, silt, and gravel in active but poorly defined drainage channels on floodplains (GSWA, 2020).

Methodology

The gold sample was photographed and weighed, and its overall morphology and external features, such as colour, roundness, surface relief, coatings, mineral inclusions and mineral assemblages were recorded using visual morphometry. The raw surface of the sample was analysed using scanning electron microscopy with energy dispersive X-ray system (SEM-EDS). The sample was then mounted in epoxy resin, cut and polished, and the gold grain microstructure and inclusions were examined using reflected-light microscopy and SEM-EDS. Gold microchemistry was determined by laser ablation inductively coupled plasma mass spectrometry (LA-ICP-MS), calibrated against certified gold reference materials (CRM; Murray, 2009). The sample was ablated in quadruplicate along 0.5 mm-long traverses and average values calculated for elements present in the CRM. The gold surface was repolished after laser ablation, cleaned using ion beam milling, and its internal structure analysed using scanning electron microscopy with electron back-scattered diffraction (SEM-EBSD). Details of this method are described in Hancock and Beardsmore (2020).

Morphology

The gold nugget is dark- brown and has irregular, -elongated, slightly flattened and rounded shape, with dimensions $12 \times 8 \times 4$ mm. It is covered by non-compacted ferruginous clays, and rare, partly oxidized pyrite grains are also present (Fig. 1).

SEM-EDS analysis of raw surfaces

The surface of nugget is spongy to flaky and intensely scratched and pitted but shows no compaction (Fig. 2a). Micro-porosity in the surface is a result of irregular dissolution of the sample rim (Fig. 2b).

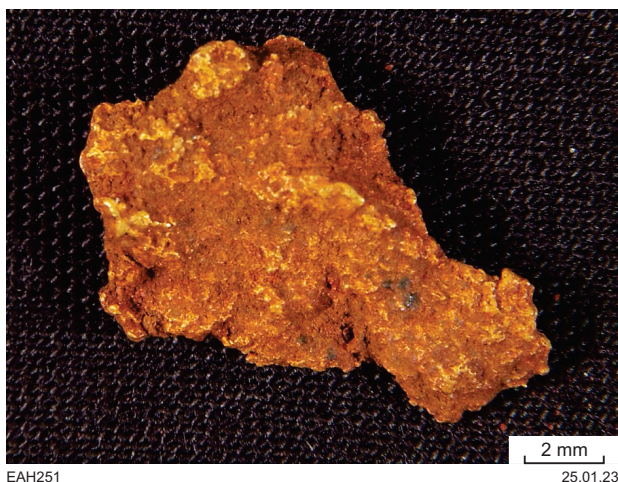


Figure 1. Sample 201980: gold nugget, Silica Hills prospect

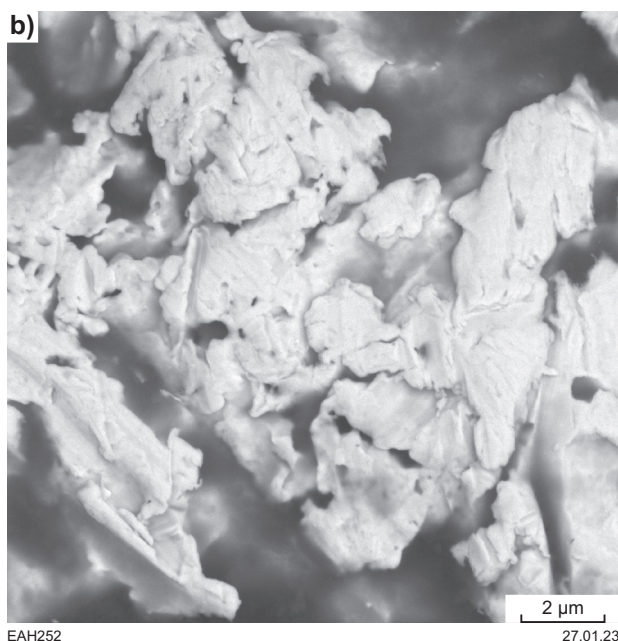
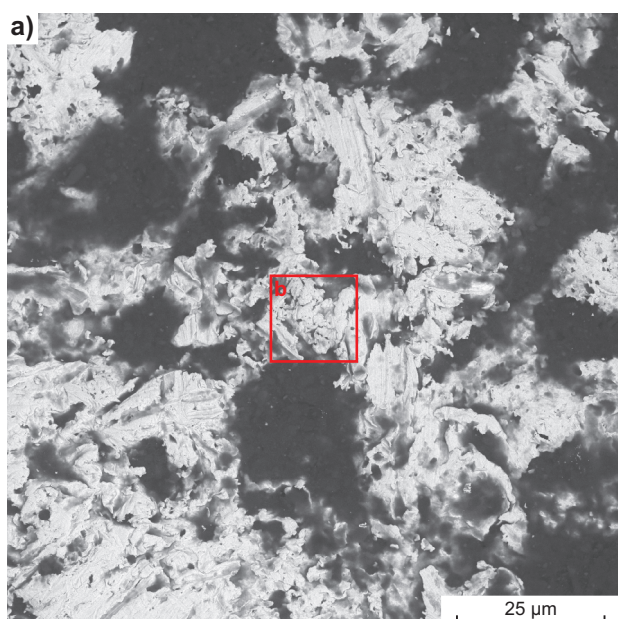


Figure 2. Backscattered electron images of parts of surface of sample 201980: gold grain, Silica Hills prospect

Optical microscopy of polished surfaces

The irregular shape and solution-pitted surface of the gold nugget is clearly evident in the polished section, as are the many large cracks and voids that penetrate the grain and are now filled with ferruginous clays and small, rounded quartz grains (Fig. 3). The voids are inferred to have formed by preferential dissolution of Ag-depleted intergranular gold veinlets. There are several partially weathered, 200 µm wide, cubic pyrite crystals on the grain margin, and some rounded galena grains <100 µm in diameter inside the sample.

SEM-EDS analysis of polished surfaces

The bulk of the gold grain contains 22% Ag, but narrow intergranular veinlets have only 1.5% Ag (Fig. 4a). There is Fe–Mg chlorite and chalcopyrite nano-inclusions in one of the rounded galena inclusions. Pyrite crystals are partially replaced by Fe±Mn oxide minerals. Voids in the gold nugget are filled with finely granular quartz and Fe-rich clays, and gold nanoparticles are disseminated in the latter (Fig. 4b).

LA-ICP-MS analysis

Ag, Cu and Hg were consistently detected within the gold grain in concentrations higher than the instrument detection limit, and probably occur as limited solid solutions in the gold. The bulk of the gold grain contains abundant Ag (15–21%), and low Cu (48–84 ppm) and Hg (98–119 ppm; Table 1). Mg and Bi are also ubiquitous, albeit just above detection of limits in some laser ablation traverses (Table 1). Zn, Sn, Sb, and Pb were detected generally in sub-ppm concentrations under detection limits (Table 2), and some lithophile elements, such as Al, Cr, Sr, and Nb, do not have available standards. All these elements likely occur in micro- and nano-inclusions.

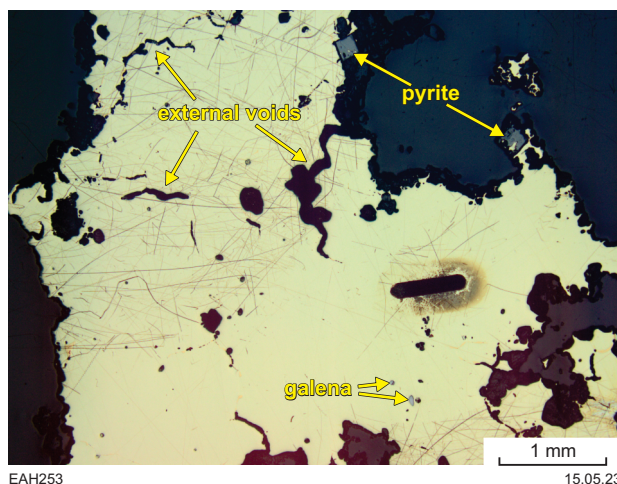


Figure 3. Reflected-light photomicrograph of cut and polished sample 201980: gold grain, Silica Hills prospect. Dark, elongate lines are laser ablation tracks produced during LA-ICP-MS analyses

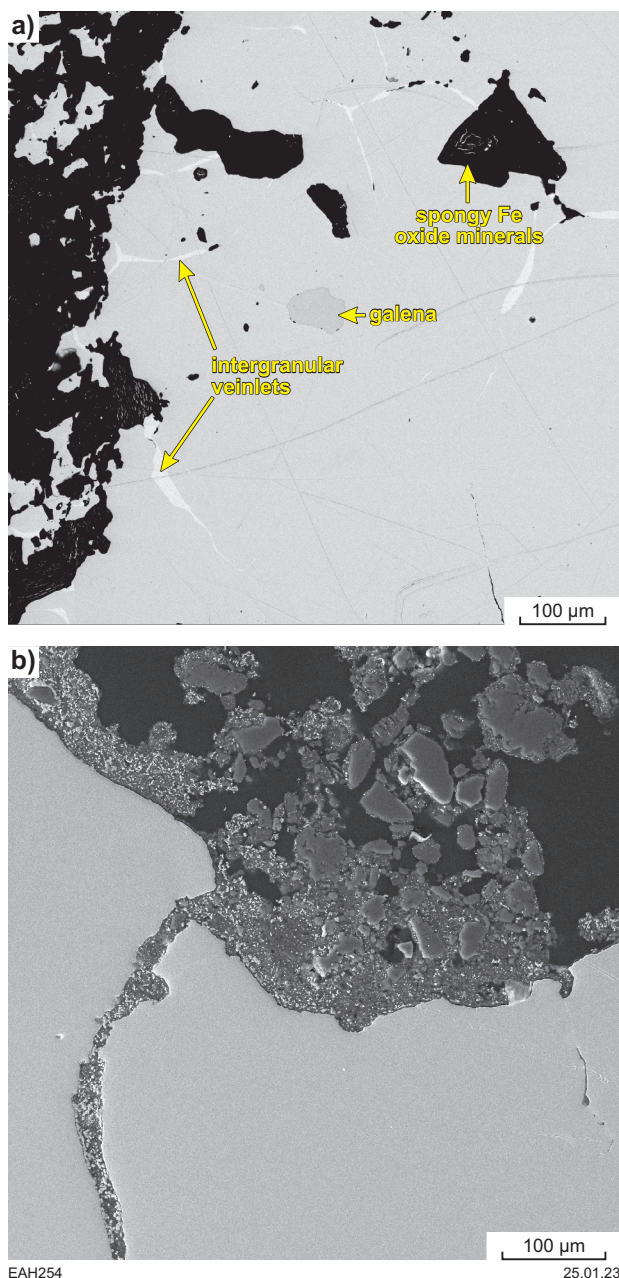


Figure 4. Backscattered electron (BSE) and secondary electron (SE) images of polished surface of sample 201980: gold grain, Silica Hills prospect: a) BSE; b) SE

Acid etching

Aqua regia was not used as an etching agent in this case because it would have reacted strongly with the abundant Ag in the gold to form an obscuring AgCl 'passivation' film. Etching was instead effected with a CrO₃-in-HCl solution, which produced red and green zones with diffused mutual contacts across much of the polished surface (Fig. 5a).

Ag-poor, bright yellow gold is evident in numerous narrow veinlets picking out the polygranular fabric of the gold, and in thin, discontinuous rims along the surface of the grain (Fig. 5a,b). Both features were formed by Ag dissolution and gold recrystallization after primary gold formation. Several small, partly weathered pyrite crystals inside the nugget are in contact with intergranular gold veinlets that extend to the grain margin, suggesting that the latter denote fractures along which oxidizing fluids were able to penetrate the grain interior (Fig. 5b).

Interpretation

Primary hydrothermal gold is coarsely granular, has high- Ag and low Cu and Hg abundances, with small inclusions of galena and pyrite. High Ag content and depletion of other trace elements are result of crystallization from low-temperature hydrothermal solutions carrying probably silver chloride complexes. The nugget was subsequently released to the surface by uplift and erosion, then buried in the regolith, where the narrow, Ag-poor intergranular veinlets and surficial rims have formed during weathering.

Table 1. LA-ICP-MS data for main elements (above detection limit) in three traverses for sample GSWA 201980: gold nugget, Silica Hills prospect

Ag (%)	Cu (ppm)	Hg (ppm)	Other elements (ppm ¹) ²
15	48	100	Bi
18	84	98	
21	83	119	Mg

NOTES: 1 See Table 2 for concentrations and detection limit
2 Results are only shown where standards are available for the element

Table 2. LA-ICP-MS compositional data for sample GSWA 201980: gold nugget, Silica Hills prospect

<i>Laser ablation track</i>	<i>Unit</i>	⁷ Li	⁹ Be	¹¹ B	²³ Na	²⁵ Mg	²⁷ Al	²⁹ Si	⁴⁴ Ca	⁴⁵ Sc	⁴⁹ Ti	⁵¹ V	⁵³ Cr	⁵⁵ Mn	⁵⁷ Fe	⁵⁹ Co	⁶⁰ Ni	⁶⁵ Cu	
1	cps			24		229	383		24	2	3		69				5	5895	
2	cps					174	247				4		53				4	10419	
3	cps			7		302	563				7	1	33			3	23	10246	
1	ppm					2.74					0.07						0.05	48	
2	ppm					2.08					0.09						0.04	84	
3	ppm					3.62					0.14						0.23	83	
<i>DL*</i>	<i>ppm</i>					3.3					1.5		1.7	1.1	3.4		2.9	1.5	
<i>Laser ablation track</i>	<i>Unit</i>	⁶⁶ Zn	⁶⁹ Ga	⁷² Ge	⁷⁵ As	⁸² Se	⁸⁵ Rb	⁸⁸ Sr	⁸⁹ Y	⁹⁰ Zr	⁹³ Nb	⁹⁸ Mo	¹⁰¹ Ru	¹⁰³ Rh	¹⁰⁸ Pd	¹⁰⁹ Ag	¹¹¹ Cd	¹¹⁵ In	
1	cps	25	3				3	24			28			1	5	31639209	2		
2	cps	22			4		1	12			27				7	36935965			
3	cps	32	5		3		11	19		3	71	1	1		5	43300525	1	3	
1	ppm	0.28													0.03	153514			
2	ppm	0.25			0.05										0.05	179214			
3	ppm	0.36			0.03										0.04	210095			
<i>DL*</i>	<i>ppm</i>	5.3			2	3.1								1.5	1.8	2.4			
<i>Laser ablation track</i>	<i>Unit</i>	¹²⁰ Sn	¹²¹ Sb	¹²⁶ Te	¹³³ Cs	¹³⁸ Ba	¹³⁹ La	¹⁴⁰ Ce	¹⁴¹ Pr	¹⁴⁵ Nd	¹⁵¹ Eu	¹⁵⁷ Gd	¹⁵⁹ Tb	¹⁶² Dy	¹⁶⁵ Ho	¹⁶⁷ Er	¹⁶⁹ Tm	¹⁷² Yb	
1	cps	22	378	2	4	9					1								2
2	cps	22	182			4											1		
3	cps	33	260		3	9	2		2	2									
1	ppm	0.10	1.47	0.03															
2	ppm	0.10	0.71																
3	ppm	0.15	1.01																
<i>DL*</i>	<i>ppm</i>	1.6	2.8	5.6															
<i>Laser ablation track</i>	<i>Unit</i>	¹⁷⁵ Lu	¹⁷⁸ Hf	¹⁸¹ Ta	¹⁸² W	¹⁸⁵ Re	¹⁸⁹ Os	¹⁹³ Ir	¹⁹⁵ Pt	²⁰² Hg	²⁰⁵ Tl	²⁰⁸ Pb	²⁰⁹ Bi	²³² Th	²³⁸ U				
1	cps			7			1			29041		20	1404		2				
2	cps			2						28437		3	15		3				
3	cps			7			1			34495	1	43	19	1	4				
1	ppm									100		0.06	2.99						
2	ppm									98		0.01	0.03						
3	ppm									119		0.13	0.04						
<i>DL*</i>	<i>ppm</i>								2.5	2.5		1.5	2.2						

NOTES: cps, count per second; ppm, parts per million; DL, detection limit

*Detection limits have been determined using AuRM Reference Gold Standards (London Bullion Market Association). Standards were analysed nine times each and an average 2σ (95% Confidence Interval) Limit of Detection determined. Some results given in the text are quoted as values that are below the detection limit for these analytes. These values must be considered as "for information" only.

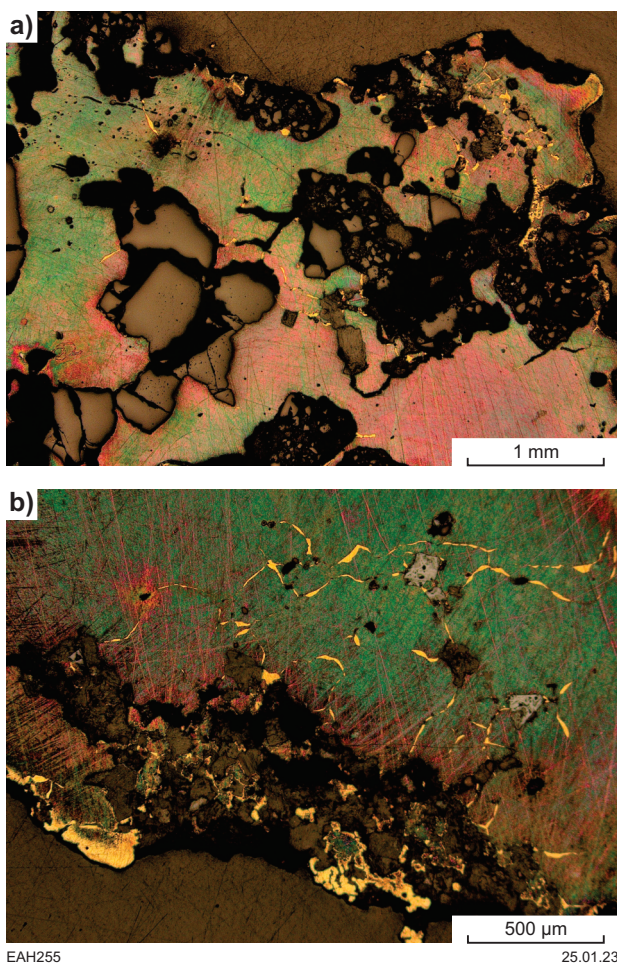


Figure 5. Reflected-light photomicrographs, after repolishing and acid etching, of sample 201980: gold grain, Silica Hills prospect

Acknowledgements

The authors gratefully acknowledge Michael Verrall (CSIRO) for his help with the SEM-EDS operation and data interpretation. We thank Professor John Watling for discussions to improve the LA-ICP-MS data interpretation.

References

- Artemis Resources Limited 2017, High Grade Gold Mineralisation identified at Silica Hills; Karratha, Western Australia (media release): Australian Securities Exchange (ASX), released 28 August 2017, 6p.
- Bob Clyne and Associates 1988, Brady's Prospect, Final Surrender Report for the period 21/02/1986 to 29/06/1990, P47/400 prepared for Mr R Brady: Geological Survey of Western Australia, Statutory mineral exploration report A27188, <www.demirs.wa.gov.au/wamex>, 58p.
- Geological Survey of Western Australia 2020, Northwest Pilbara, 2020: Geological Survey of Western Australia, Geological Information Series, data package (USB).
- Hancock, EA and Beardsmore, TJ 2020, Provenance fingerprinting of gold from the Kurnalpi Goldfield: Geological Survey of Western Australia, Report 212, 21p.
- Hickman, AH 2016, Northwest Pilbara Craton: A record of 450 million years in the growth of Archean continental crust: Geological Survey of Western Australia, Report 160, 104p.
- Hickman, AH 2021, Tozer Formation (A-WHt-xb-f): Geological Survey of Western Australia, WA Geology Online, Explanatory Notes extract, viewed 04 January 2023, <www.demirs.wa.gov.au/ens>.
- Murray, S 2009, LBMA certified reference materials. Gold project final update: The London Bullion Market Association, Alchemist, no. 55, p. 11–12.

Recommended reference for this publication

- Hancock, EA, Blay, OA and Beardsmore, TJ 2025, 201980: gold nugget, Silica Hills prospect; GSWA Mineralogy Record 14: Geological Survey of Western Australia, 5p.